

## Photoelectrochemical Reduction of Carbon Dioxide at Si(111) Electrode Modified by Viologen Molecular Layer with Metal Complex

Yu Sun,<sup>1</sup> Takuya Masuda,<sup>2</sup> and Kohei Uosaki\*<sup>1,2,3</sup>

<sup>1</sup>Division of Chemistry, Graduate School of Science, Hokkaido University, Sapporo, Hokkaido 060-0810

<sup>2</sup>Global Research Center for Environment and Energy based on Nanomaterials Science (GREEN),  
National Institute for Materials Science (NIMS), Tsukuba, Ibaraki 305-0044

<sup>3</sup>International Center for Materials Nanoarchitectonics (MANA), National Institute for Materials Science (NIMS),  
Tsukuba, Ibaraki 305-0044

(Received November 24, 2011; CL-111128; E-mail: uosaki.kohei@nims.go.jp)

Photoelectrochemical carbon dioxide reduction was carried out at a p-type Si(111) electrode modified with a viologen molecular layer and  $[\text{AuCl}_4]^-$  or  $[\text{PdCl}_4]^{2-}$ . It was proven that the reduction reaction was mediated by viologen moiety and while  $\text{CO}_2$  reduction was dominant at the Si(111) electrode modified with  $[\text{PdCl}_4]^{2-}$  in the potential region where viologen moiety was in the first reduced state, it became dominant at the electrode modified with  $[\text{AuCl}_4]^-$  when viologen moiety became the second reduced state. FT-IR measurement confirmed the formation of formic acid/formate ion at the  $[\text{PdCl}_4]^{2-}$ /viologen-modified Si electrode.

Carbon dioxide fixation attracts much interest of many scientists and engineers not only because  $\text{CO}_2$  is considered to be one of the main causes of global warming<sup>1</sup> but also because it is scientifically very challenging to convert  $\text{CO}_2$ , one of the most stable molecules, to fuels and useful chemicals.<sup>2</sup> Electrochemical reduction of  $\text{CO}_2$  is one of the most studied systems,<sup>2-4</sup> but very large overpotential and low current efficiency prevent its practical use. Moreover, if electricity is generated by using fossil fuel, more  $\text{CO}_2$  is produced. Photoelectrochemical and photocatalytic reduction of  $\text{CO}_2$  using a semiconductor is ideal as solar energy can be utilized to reduce  $\text{CO}_2$ .<sup>2</sup> Unfortunately, however, most of the semiconductors, which have a suitable band gap for solar energy conversion, are corrosive in aqueous solutions.<sup>5</sup> Furthermore, most of the semiconductor surfaces are not catalytically active for multi-electron-transfer reactions such as hydrogen evolution and  $\text{CO}_2$  reduction, because they do not adsorb reaction intermediates with suitable strength.<sup>6-8</sup> One method to solve these problems is to modify the semiconductor surface with metal or metal ions, which act as catalyst. But this approach has one severe problem that surface states, which act as charge recombination centers, are often introduced at the metal-semiconductor interface as a result of the surface modification by metal.<sup>9</sup>

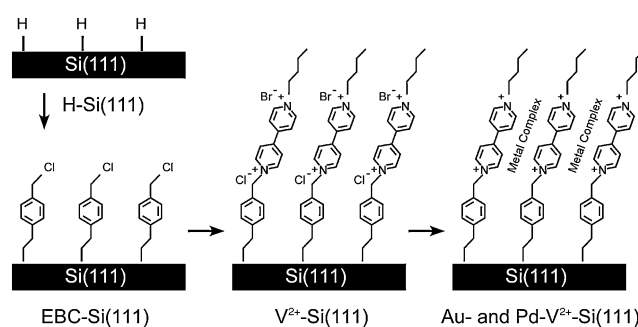
Several groups have used organic molecular layers to separate catalytic metals and semiconductor surfaces so that the introduction of surface states, which is the result of direct contact between catalytic metals and semiconductor surface, can be avoided and demonstrated that efficiencies of photoelectrochemical reactions are significantly enhanced, although the position and amount of catalyst are not well controlled.<sup>8d,10,11</sup> Recently, we have demonstrated that very efficient photoelectrochemical hydrogen evolution reaction (HER) can be achieved at a Si(111) electrode modified with a highly ordered organic molecular layer with viologen moieties, which is directly

bonded to Si surface via Si-C bond, as an electron mediator and Pt complex, which is confined within the molecular layer as a catalyst.<sup>12,13</sup>

In this paper, we have extended this approach to photoelectrochemical carbon dioxide reduction at p-type Si(111) electrode modified with viologen molecular layer and various metal complexes.  $[\text{AuCl}_4]^-$  and  $[\text{PdCl}_4]^{2-}$  are chosen as complexes as electrochemical  $\text{CO}_2$  reduction is known to proceed efficiently at Au and Pd electrodes while  $\text{H}_2$  generation is dominant at Pt electrode in  $\text{CO}_2$ -saturated solution.<sup>14</sup>

Surface modification was carried out as schematically shown in Scheme 1. Details of the procedure for the modification by organic layers and characterization of modified surfaces have been reported before.<sup>12</sup> Briefly, a freshly prepared hydrogen-terminated (H-) Si(111) surface<sup>15</sup> was sequentially treated to yield a viologen monolayer-modified ( $\text{V}^{2+}$ -) Si(111) substrate: (1) H-Si(111) surface was illuminated with 254-nm light for 2 h in deaerated 4-vinylbenzyl chloride to yield a 4-ethylbenzyl chloride-modified (EBC-) Si(111) surface, (2) the substrate was then kept in benzene solution saturated with 4,4'-bipyridine and then in 1-bromobutane, both at 70 °C for 12 h to obtain a  $\text{V}^{2+}$ -Si(111) surface. The  $\text{V}^{2+}$ -Si(111) was immersed in an aqueous solution containing 10 mM of  $[\text{AuCl}_4]^-$  or  $[\text{PdCl}_4]^{2-}$  for 20 min at room temperature to yield Au- or Pd- $\text{V}^{2+}$ -Si(111) surfaces, respectively.

X-ray photoelectron spectra (XP spectra) obtained using a Rigaku model XPS-7000 with monochromic Mg K $\alpha$  for the (A) Au- and (B) Pd- $\text{V}^{2+}$ -Si(111) surfaces in Au4f and Pd3d regions, respectively, confirm the incorporation of the metals.<sup>16</sup>



**Scheme 1.** Schematic illustration of the modification steps of hydrogen-terminated (H-) Si(111) surface to obtain Au- and Pd- $\text{V}^{2+}$ -Si(111) surfaces. Metal Complex:  $[\text{AuCl}_4]^-$  and  $[\text{PdCl}_4]^{2-}$ . See the text for the detail.<sup>12</sup>

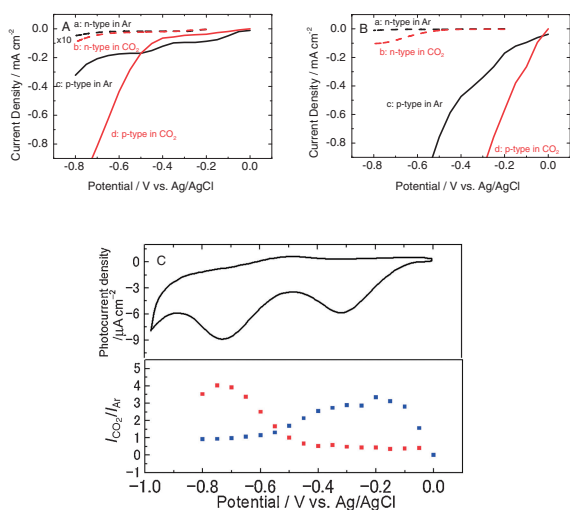


**Figure 1.** Current–voltage relations of (A) Au- and (B) Pd-V<sup>2+</sup>-Si(111) electrodes in 0.1 M aqueous Na<sub>2</sub>SO<sub>4</sub> solutions saturated with Ar (black; a, c) and CO<sub>2</sub> (red; b, d) in dark (n-type, broken line; a, b) and under illumination (p-type, solid line; c, d) with a light intensity of 0.12 mW cm<sup>-2</sup>. Scan rate: 1 mV s<sup>-1</sup>. (C) Top panel: Cyclic voltammogram of p-type V<sup>2+</sup>-Si(111) electrode in a 0.1 M aqueous Na<sub>2</sub>SO<sub>4</sub> solution saturated with Ar under illumination with a light intensity of 0.12 mW cm<sup>-2</sup>. Scan rate: 100 mV s<sup>-1</sup>. Bottom panel: Ratio between currents at Au- (red) and Pd-V<sup>2+</sup>-Si(111) electrodes (blue) in CO<sub>2</sub>-saturated solution and that in Ar-saturated solution ( $I_{\text{CO}_2}/I_{\text{Ar}}$ ) as a function of potential.

Figure 1 shows  $I$ - $V$  curves of the (A) Au- and (B) Pd-V<sup>2+</sup>-Si(111) electrodes in Ar- and CO<sub>2</sub>-saturated 0.1 M aqueous Na<sub>2</sub>SO<sub>4</sub> solutions. The pH of the Ar-saturated 0.1 M Na<sub>2</sub>SO<sub>4</sub> solution was adjusted to 4.4 by adding H<sub>2</sub>SO<sub>4</sub>, since the pH of 0.1 M Na<sub>2</sub>SO<sub>4</sub> changed from 5.9 to 4.4 by CO<sub>2</sub> saturation. Relatively small current flowed at the n-Si(111) electrodes modified with viologen layer/metal complexes in the dark both in Ar- and CO<sub>2</sub>-saturated solutions. However, currents in CO<sub>2</sub>-saturated solution were clearly larger than those in Ar-saturated solution at potentials more negative than ca. -0.5 V.

Cathodic currents in both the Ar- and CO<sub>2</sub>-saturated solutions started to flow at much more positive potentials at the p-Si(111) electrodes modified with viologen layer/metal complexes under illumination<sup>17</sup> than those at the modified n-Si(111) electrode in the dark, although only negligibly small currents flowed in the dark (<5 μA cm<sup>-2</sup> at -0.8 V) as expected because electrons are the minority carrier of p-type semiconductors. At the p-type Pd-V<sup>2+</sup>-Si(111) electrode, photocurrent started to flow at potential as positive as 0 V and increased significantly as potential became more negative both in the Ar- and CO<sub>2</sub>-saturated solutions. Photocurrent in the CO<sub>2</sub>-saturated solution was larger than that in the Ar-saturated solution in the potential region shown in Figure 1, but both became almost the same as potential became more negative than ca. -0.6 V. On the other hand, although photocurrent started to flow also at around 0 V at the Au-V<sup>2+</sup>-p-Si(111) electrode in both solutions, it did not increase much even when potential was made more negative, particularly in the Ar-saturated solution. Photocurrent in the CO<sub>2</sub>-saturated solution significantly increas-

ed and became larger than that in the Ar-saturated solution when potential became more negative than ca. -0.55 V.

These trends are more clearly seen in the bottom panel of Figure 1C, which shows potential dependencies of the ratio between photocurrents in the CO<sub>2</sub> ( $I_{\text{CO}_2}$ ) and Ar-saturated solutions ( $I_{\text{Ar}}$ ) at the Au-V<sup>2+</sup>- and Pd-V<sup>2+</sup>-Si(111) electrodes. At the Pd-modified Si electrode,  $I_{\text{CO}_2}$  became larger than  $I_{\text{Ar}}$  as soon as photocurrent started to flow at 0 V, but  $I_{\text{CO}_2}/I_{\text{Ar}}$  gradually decreased as potential became more negative than ca. -0.2 V and became 1 as potential became more negative than ca. -0.6 V as mentioned before. At the Au-modified Si electrode,  $I_{\text{CO}_2}$  was smaller than  $I_{\text{Ar}}$  in the relatively positive potential region, but  $I_{\text{CO}_2}/I_{\text{Ar}}$  increased significantly as potential became more negative than ca. -0.5 V and reached 4 at -0.7 V. The top panel of Figure 1C is the cyclic voltammogram (CV) of V<sup>2+</sup>-Si(111) electrode without metal complex under illumination obtained with very fast scan rate (50 mV s<sup>-1</sup>). Reduction peaks of viologen moiety are clearly observed at -0.25 and -0.7 V for the reduction of V<sup>2+</sup> to V<sup>•+</sup> and of V<sup>•+</sup> to V<sup>••</sup>, respectively. Positions of these peaks were more positive than those observed at n-type V<sup>2+</sup>-Si(111) electrode in the dark as expected.<sup>12b</sup> Potential dependencies of photocurrent and  $I_{\text{CO}_2}/I_{\text{Ar}}$  seem to be related to the reduced state of viologen moiety. While at the Pd-V<sup>2+</sup>-Si(111) electrode, large photocurrent flowed in both Ar- and CO<sub>2</sub>-saturated solution as soon as the reduction of V<sup>2+</sup> to V<sup>•+</sup> started, at the Au-V<sup>2+</sup>-Si(111) electrode, only relatively small and almost no photocurrent were observed in Ar- and CO<sub>2</sub>-saturated solutions, respectively, in potential region where viologen moiety was in V<sup>•+</sup>, and significant increase of photocurrent was observed in CO<sub>2</sub>-saturated solution as soon as V<sup>•+</sup> was reduced to V<sup>••</sup>. This difference should be due to the difference in the energy to form adsorbed intermediate states on the metal catalysts.

As a qualitative analysis of the products of CO<sub>2</sub> reduction, in situ FT-IR measurements were performed at the Au- and Pd-V<sup>2+</sup>-Si(111) electrodes in 0.1 M Na<sub>2</sub>SO<sub>4</sub> solution saturated with CO<sub>2</sub>.<sup>18</sup> Figure 2A shows IR spectra (s-polarization) obtained at the Pd-V<sup>2+</sup>-Si(111) electrode in the CO<sub>2</sub>-saturated 0.1 M Na<sub>2</sub>SO<sub>4</sub> solution keeping the potential at -0.7 V for a given period of time under illumination with a spectrum measured in dark before illumination as a reference.

No significant difference was noticed between the p- and s-polarized spectra.<sup>20</sup> Negative peaks due to the consumption in the thin layer were observed at around 1600, 2350, and 3200 cm<sup>-1</sup>, corresponding to bending of OH of water, CO stretching of dissolved CO<sub>2</sub>, and OH stretching of water, respectively, showing that HER and CO<sub>2</sub> reduction proceeded. A small positive peak due to the accumulation of reduction product was observed at around 1410 cm<sup>-1</sup>, which corresponds to symmetric stretch of carboxylate group. The growth of this peak with time is more clearly seen in Figure 2B, which shows IR spectra in 1325–1475 cm<sup>-1</sup> region with correction of background due to a strong negative OH bending peak. This agrees with previous reports that the main product of electrochemical carbon dioxide reduction reaction at Pd electrode is formic acid/formate ion.<sup>21</sup> Asymmetric stretching peak of carboxylate group, which should be present at around 1610 cm<sup>-1</sup> is not visible because of a strong negative OH bending peak at this potential. IR spectra obtained at various potentials shown in Figure 2C indicate that at -0.2 V, the negative OH bending peak is

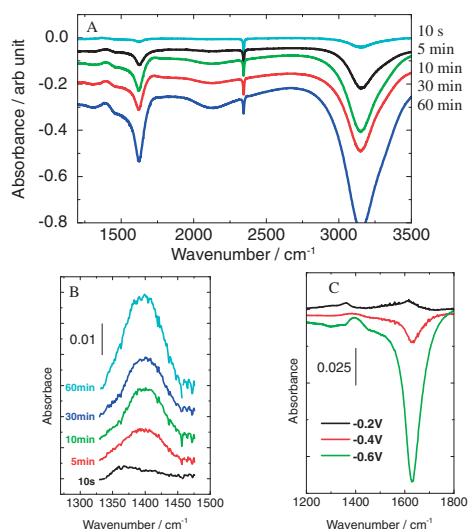


**Figure 2.** IR spectra at the Pd- $V^{2+}$ -Si(111) electrode in a  $CO_2$ -saturated 0.1 M  $Na_2SO_4$  solution (A, B) with keeping the potential at  $-0.7$  V for a given period of time under illumination in (A) 1250–3500 and (B) 1325–1475  $cm^{-1}$  regions with background correction, and (C) at various potentials in 1200–1800  $cm^{-1}$  region.

not visible and that small positive peaks due to symmetric and asymmetric stretch of carboxylate are observed. This is in good agreement with the result shown in Figure 1B that the dominant reaction at this potential is  $CO_2$  reduction.

In situ FT-IR measurements obtained at the Au- $V^{2+}$ -Si(111) electrode in 0.1 M  $Na_2SO_4$  solution saturated with  $CO_2$  shows only negative peaks due to the consumption in the thin layer at around 1600, 2350, and 3200  $cm^{-1}$ , corresponding to bending of OH of water, CO stretching of dissolved  $CO_2$ , and OH stretching of water, respectively, and no positive peaks were observed. Thus, although it is confirmed that HER and  $CO_2$  reduction proceeded at the Au- $V^{2+}$ -Si(111) electrode, no product was determined. According to previous reports, the main product of  $CO_2$  reduction at gold electrode is  $CO$ .<sup>14</sup>

In conclusion, photoelectrochemical carbon dioxide reduction was significantly enhanced by modifying Si(111) surfaces by the organic molecular layer with viologen moieties and  $[AuCl_4]^-$  or  $[PdCl_4]^{2-}$ . It was confirmed that viologen moiety plays an important role for mediating electron transfer from Si to metal catalysts. While  $CO_2$  reduction was dominant at the Si(111) electrode modified with  $[PdCl_4]^{2-}$  in the potential region where viologen moiety was in the first reduced state, the second reduced state is required to reduce  $CO_2$  at the electrode modified with  $[AuCl_4]^-$ . FT-IR measurements confirmed the formation of formic acid/formate ion as a product of  $CO_2$  reduction, and selectivity of  $CO_2$  reduction to HER is high at the positive potential at Pd- $V^{2+}$ -Si(111) electrode. The decrease of selectivity for  $CO_2$  reduction at the Pd- $V^{2+}$ -Si(111) electrode as potential became negative should simply be due to the low surface concentration of  $CO_2$  with respect to  $H_2O$  ( $H^+$ ) for HER. More detailed analysis including gaseous products is under way.

Professors Katsuaki Shimazu and Toshikazu Kawaguchi are acknowledged for XPS measurements. The present work was partially supported by GCOE Program (Project No. B01:

Catalysis as the Basis for Innovation in Materials Science), World Premier International Research Center (WPI) Initiative on Materials Nanoarchitectonics, and MEXT Program for Development of Environmental Technology using Nanotechnology from Ministry of Education, Culture, Sports, Science and Technology, Japan. YS is supported by MEXT scholarship for foreign students.

## References and Notes

- 1 J. O'M. Bockris, *Energy Options: Real Economics and the Solar-Hydrogen System*, Halsted, New York, **1980**.
- 2 M. M. Halmann, *Chemical Fixation of Carbon Dioxide: Methods for Recycling  $CO_2$  into Useful Products*, CRC, Florida, **1993**, Chap. 8, pp. 121–127.
- 3 M. Mikkelsen, M. Jørgensen, F. C. Krebs, *Energy Environ. Sci.* **2010**, *3*, 43.
- 4 Y. Hori, in *Modern Aspects of Electrochemistry*, ed. by C. G. Vayenas, R. E. White, M. E. Gamboa-Aldeco, Springer, New York, **2008**, Vol. 42, Chap. 3, pp. 89–189. doi:10.1007/978-0-387-49489-0-3.
- 5 A. J. Nozik, *Annu. Rev. Phys. Chem.* **1978**, *29*, 189.
- 6 J. O'M. Bockris, K. Uosaki, *J. Electrochem. Soc.* **1977**, *124*, 1348.
- 7 K. Uosaki, H. Kita, in *Modern Aspects of Electrochemistry*, ed. by B. E. Conway, J. O'M. Bockris, R. E. White, Springer, New York, **1986**, Vol. 18, Chap. 3, pp. 1–60.
- 8 a) Y. Nakato, S. Tonomura, H. Tsubomura, *Ber. Bunsen-Ges. Phys. Chem.* **1976**, *80*, 1289. b) W. Kautek, J. Gobrecht, H. Gerischer, *Ber. Bunsen-Ges. Phys. Chem.* **1980**, *84*, 1034. c) A. Heller, *Acc. Chem. Res.* **1981**, *14*, 154. d) R. N. Dominey, N. S. Lewis, J. A. Bruce, D. C. Bookbinder, M. S. Wrighton, *J. Am. Chem. Soc.* **1982**, *104*, 467. e) F.-R. F. Fan, R. G. Keil, A. J. Bard, *J. Am. Chem. Soc.* **1983**, *105*, 220. f) K. Uosaki, H. Kita, *Chem. Lett.* **1984**, 301. g) M. Szklarczyk, J. O'M. Bockris, *J. Phys. Chem.* **1984**, *88*, 5241.
- 9 a) Y. Nakato, K. Ueda, H. Yano, H. Tsubomura, *J. Phys. Chem.* **1988**, *92*, 2316. b) K. Uosaki, Y. Shigematsu, H. Kita, *Chem. Lett.* **1988**, 1815. c) K. Uosaki, Y. Shigematsu, S. Kaneko, H. Kita, *J. Phys. Chem.* **1989**, *93*, 6521.
- 10 D. C. Bookbinder, J. A. Bruce, R. N. Dominey, N. S. Lewis, M. S. Wrighton, *Proc. Natl. Acad. Sci. U.S.A.* **1980**, *77*, 6280.
- 11 a) K. Nakato, S. Takabayashi, A. Imanishi, K. Murakoshi, Y. Nakato, *Sol. Energy Mater. Sol. Cells* **2004**, *83*, 323. b) S. Takabayashi, M. Ohashi, K. Mashima, Y. Liu, S. Yamazaki, Y. Nakato, *Langmuir* **2005**, *21*, 8832.
- 12 a) T. Masuda, K. Uosaki, *Chem. Lett.* **2004**, *33*, 788. b) T. Masuda, K. Shimazu, K. Uosaki, *J. Phys. Chem. C* **2008**, *112*, 10923.
- 13 T. Masuda, H. Fukumitsu, S. Takakusagi, W.-J. Chun, T. Kondo, K. Asakura, K. Uosaki, *Adv. Mater.* **2012**, *24*, 268.
- 14 a) Y. Hori, H. Wakebe, T. Tsukamoto, O. Koga, *Electrochim. Acta* **1994**, *39*, 1833. b) M. Azuma, K. Hashimoto, M. Hiramoto, M. Watanabe, T. Sakata, *J. Electrochem. Soc.* **1990**, *137*, 1772.
- 15 S. Ye, T. Ichihara, K. Uosaki, *Appl. Phys. Lett.* **1999**, *75*, 1562.
- 16 G. E. Muilenberg, *Handbook of X-ray Photoelectron Spectroscopy*, Perkin-Elmer, Minnesota, **1978**.
- 17 Illumination was provided by a 500-W xenon lamp (Ushio, UXL-500-D) through an IR cut filter (Toshiba, IRA-20), a UV cut filter (Sigma Koki) and an ND filter (Toshiba).
- 18 ATR FT-IR spectra were obtained in thin layer configuration<sup>19</sup> using a Bio-Rad FTS-30 spectrometer equipped with a mercury cadmium telluride (HgCdTe) detector cooled with liquid nitrogen. A diode laser (13 mW  $cm^{-2}$ ) was used as a light source. All the spectra were measured by integrating 32 interferograms with a resolution of 2  $cm^{-1}$ .
- 19 K. Uosaki, Y. Shigematsu, H. Kita, K. Kunimatsu, *J. Phys. Chem.* **1990**, *94*, 4623.
- 20 It must be noted the nonzero contribution of surface species in s-polarized IR spectra at semiconductor electrode, although s-polarized IR spectra at metal electrode contains no information from the surface species.<sup>19</sup>
- 21 a) K. Ohkawa, K. Hashimoto, A. Fujishima, Y. Noguchi, S. Nakayama, *J. Electroanal. Chem.* **1993**, *345*, 445. b) K. Ohkawa, Y. Noguchi, S. Nakayama, K. Hashimoto, A. Fujishima, *J. Electroanal. Chem.* **1994**, *369*, 247.